The Disk Wind Contribution to the Optical Spectra of Cataclysmic Variables

J. H. Matthews, C. Knigge, K. S. Long, S. A. Sim & N. Higginbottom

10 February 2014

ABSTRACT

High-State non-magnetic Cataclysmic Variable systems (CVs) exhibit strong emission in Hydrogen & Helium optical recombination lines. Here we present results obtained by encorporating a macro atom treatment into our Monte Carlo radiative transfer code originally used to model UV resonance lines in CVs, Python . Our benchmark CV model is capable of producing all of the notable optical lines (e.g. He II 4686, Hα, He I), as well as enchanced emission in the Ly-α and He II 1640 UV lines. In addition, the improved treatment of recombination means that the bound-free continuum emission is sufficient to mask the so-called 'Balmer jump' photoabsorption edge, suggesting a potential solution to a longstanding problem.

1 INTRODUCTION

Non-magnetic Cataclysmic Variables (CVs), are systems in which a white dwarf accretes matter from a donor star through Roche-lobe overflow onto an accretion disk. It has been shown that the spectra of high state CVs exhibit absorption features believed to be caused by an outflow, potentially line-driven, rising from the accretion disk (Cordova & Mason 1982). The ultraviolet spectra of CVs, in particular, exhibit P-Cygni like profiles in resonance lines such as NV, OVI and, most commonly, CIV. This hints at the possibility of the wind being line driven, as these resonance lines must experience a line force if they are photoionised by a disk or other photon source close to the centre of the system.

Multiple attempts have been made to model UV wind spectra by treating the wind as a biconical flow arising from the accretion disk, and conducting radiative transfer simulations to attempt to reproduce the resonance lines that appear in the spectra. The first generation of models applied knowledge gleaned from stellar wind modeling to the problem (Mauche & Raymond 1987; Drew 1987; Vitello & Shlosman 1988), showing that mass loss rates of $\sim 10\%$ of the accretion rate were required to produce the required line strengths. Shlosman & Vitello (1993; hereafter SV93) describe a radiative transfer code which first computes an ionization structure based on constant wind temperature, and then used the Sobolev approximation for line transfer.

2 DESCRIPTION OF THE CODE

Python is a Monte Carlo radiative transfer code which uses the Sobolev approximation. It expands on the work of SV93 and also incorporates techniques described by Lucy (1999a, 1999b, 2002, 2003). The code is first described by Long & Knigge (2002), who synthesized the UV spectra of CVs, successfully reproducing P-Cygni resonance line profiles whilst solving self-consistently for the thermal balance and ionization structure in the wind according to the method of Mazzali & Lucy (1993). Python has since been used with application to QSO wind modeling (Higginbottom et al. 2013), which involved a new ionization scheme to deal with the more complex power-law spectrum, and encorporation os processes such as Compton scattering in order to correctly treat X-ray radiation transfer. In addition, (Sim et al. 2005) modeled Brackett and Pfund line profiles in YSOs using Python , using the macro atom scheme outlined by Lucy (2002, 2003) applied to a Hydrogen-only model.

Here, we model the UV resonance lines in much the same way as LK02, using the fast two-level atom approximation which is appropriate for treating transitions with strong coupling to the ground state. However, our model has one crucial difference to LK02, as we use the macro atom scheme in tandem with this method. Hydrogen and Helium are treated as macro atoms in an attempt to provide a better treatment of optical recombination lines (e.g. the Balmer series, He II 4686, He I lines),

Lyman-α, and the recombination continuum which is suspected to play a key role in 'filling-in' the Balmer photoionization edge (see e.g. Knigge & Drew 1998).

2.1 Macro-atoms

In its standard operating mode, Python uses a two-level atom approximation (see e.g. Mihalas 1982) for its treatment of lines. This approximation works well when treating so-called 'resonance lines' (such as C iv , Ovi), in which the excited electron is strongly coupled to the ground state, but breaks down for more complex situations such as recombination cascades. To properly model recombination lines, including the Lyman and Balmer series, a more complete treatment of line transfer is required.

Lucy (2002, 2003; hereafter L02, L03) showed that by quantising matter into 'macro-atoms', and radiant and kinetic energy into energy packets, it is possible to asymptotically reproduce the emisssivity of a gas in statistical equilibrium without simplifying line transfer. Macro-atoms are finite volume elements with internal transition probabilities that are 'activated' by packets of radiant (r-packets) or kinetic (k-packets) energy. A typical activation and deactivation sequence is shown in figure **??**. A full description is far beyond the scope of this report- consult L02 and L03.

The macro-atom scheme has been used with Python before, in a Hydrogen-only mode with application to YSOs (Sim et al. 2005), but has not yet been applied to AGN or CV problems. With some improvements, the current scheme will enable Python to model H and He recombination lines, for example. The fast, simple treatment of resonance lines can be retained, as the Python implementation allows for non-macro atom treatment for certain ions.

2.2 Atomic Data

Atomic data is obtained from the same sources described in LK02 and updated in H13. The additional level and line information required to treat Helium as macro atom was obtained from Topbase (Badnell et al. 2005). We treat Hydrogen as a 20-level atom as in S05, where each level is defined by the principal quantum number n, which is appropriate due to the degeneracy of each level in the Hydrogen atom. Helium II is treated in much the same way, with 10 levels, but He I has larger energy differentials between different l subshells and triplet and singlet states. Thus, we still include levels up to n=10 but explicitly treat the l-subshells as distinct levels instead of assuming they are perfectly 'l-mixed', which will have the pleasant side effect having the potential to produce triplet lines.

2.3 Ionization scheme

Although H13 developed a new ionization scheme which approximates the SED in a cell with a broken power law, here we follow LK02 in using the ionization scheme presented by Mazzali & Lucy (1993), who specifically present the formula

$$\frac{n_{j+1}n_e}{n_j} = W[\xi + W(1-\xi)] \left(\frac{T_e}{T_R}\right)^{1/2} \left(\frac{n_{j+1}n_e}{n_j}\right)^*_{T_R}, \quad (1)$$

which, in principle, accounts for ionizations from and recombinations to all levels of an ion. In this equation, the last ("starred") term on the right hand side refers to the Saha abundances, W is an effective dilution factor, ξ is the fraction of recombinations going directly to the ground state, and T_R and T_e are the radiation and electron temperature respectively. LK02 provide a full description of our implementation.

The reason for using this scheme is twofold; First, the SED can be approximated well by a Blackbody due to the absence of an X-ray source, and therefore the blackbody treament is appropriate; Second, this provides continuity from LK02 and allows us to do a like-for-like comparison, which is especially useful in assessing the improvement in Hydrogen line emission, and any changes that might occur in the ionization stages of the resonance line species such as CIV.

3 CODE VALIDATION AND TESTING

3.1 Ionization

LK02 presented comparisons of between Python and the widely used photoionization code Cloudy, showing good agreement of calculated ion fractions between the code. In addition, Kerzendorf & Sim (2014) present a code for spectral synthesis of Supernova (TARDIS) which compares spectra from a homologous spherical model with the ML92 ionization scheme. We are therefore confident that our treatment for so-called 'simple ions' is correct.

To verify that the macro atom treatment is correct, it is important to compare level population tests fro Hydrogen and Helium with that expected from literature. In addition, we check that the dual macro atom/simple ion implementation still shows good agreement with Cloudy.

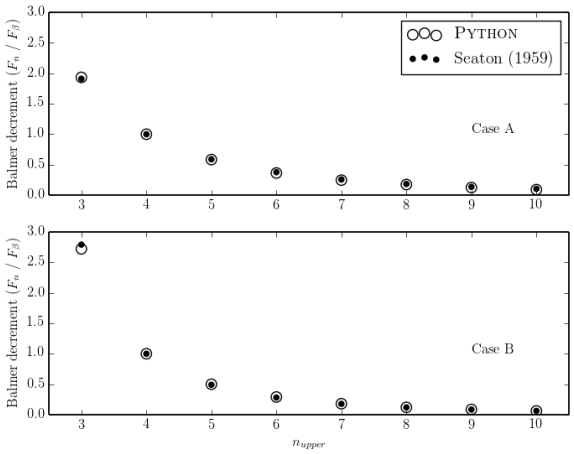

Figure 1. Case A comparison between S59 and Python at 10000K and 20000K

3.2 Non-LTE Level Populations

Before proceeding with modeling of CV systems, we need to be sure that our scheme fulfils Lucy's (2002) statement that it will 'asymptotically reproduce the emissivity of a gas in statistical equilibrium'. For our tests, we use a Hydrogen only 'thin shell' mode in Python , in which a single macro atom is created as a spherical shell with a thickness of 1cm. We construct the situation such that all opacities other than bound-free absorption are negligible, and the only cooling process available to the gas is that of recombination line emission. This is a mathematical pathology, commonly known as 'Case A', and allows us to test against analytical calculations.

As Python normally models dense environments, it assumes each principal quantum number level is well 'l-mixed' - that is each subshell of a given level is populated according to statistical weight by inelastic collisions. It is therefore not possible to compare with non-L mixed calculations such as those presented in Osterbrock (1989). Seaton (1959; S59) carried out calculations for Case A in the l-mixed case, and is thus a better comparison. Figure 1 shows a comparison between S59 and Python , showing excellent agreement. Figure 2 shows the Case B comparison, in which the escape probabilities for the Lyman lines have been explicitly zeroed.

This test verifies the treatment of recombination lines in Hydrogen only models, but it is also necessary to test the implementation of macro-atoms when other elements are treated as so-called 'simple ions'. In this mode, the user can select which species to treat as macro atoms, meaning that the other species are still treated with a two-level approximation. This means that the fast treatment of resonance lines can be maintained without sacrificing the necessity that all energy packets are indivisible. It is important to verify that this still produces the correct ionization state for the wind. We can test this by comparing against both Cloudy and LK02.

Figure 3 shows a comparison between the macro atom mode and standard mode of the code using the SV93 model. The ionization state is remarkably similar.

4 THE BENCHMARK CV MODEL

4.1 Description of Model: Geometry and Kinematics

As in LK02, we follow the prescription of SV93 in both our fundamental biconical wind model and velocity law. The poloidal velocity, v_l, along a streamline in our model is given by

$$v_l = v_0 + [v_\infty(r_0) - v_0] \frac{(l/R_v)^\alpha}{(l/R_v)^\alpha + 1}, \quad (2)$$

where l is distance measured along a poloidal streamline. This power-law velocity profile was adopted by SV93 in order to give a continuous variation in the derivative of the velocity and a realistic spread of Doppler-shifted frequencies in the outer portion of the wind ($l > R_v$). We have similar requirements. The initial poloidal velocity of the wind, v_0 is (somewhat arbitrarily) set to 6 km s^{-1} for all streamlines, comparable to the sound speed in the disk photosphere. The wind then speeds up on a characteristic scale length R_v, defined as the position along the poloidal streamline at which the wind reaches half its terminal velocity, v_∞. The terminal poloidal velocity along each streamline is set to a fixed multiple of the escape velocity at the streamline foot point,

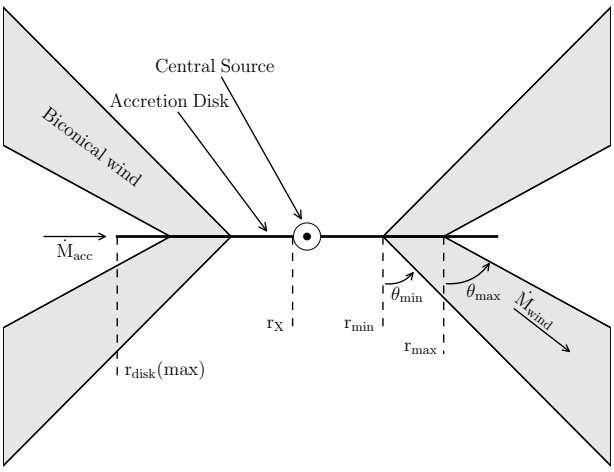

Figure 2. Cartoon illustrating the three broad classes of sightline discussed in the text.

Free Parameters	Value
M_{WD}	$0.8M_{\odot}$
$\dot{M}_{acc}$	$3.16 \times 10^{-}9\ M_{\odot}yr^{-1}$
$\dot{M}_{wind}$	$3.16 \times 10^{-}8\ M_{\odot}yr^{-1}$
r_{min}	$4R_{WD}$
r_{max}	$12R_{WD}$
θ_{min}	$20.0°$
θ_{max}	$65.0°$
λ	0
v_{∞}	$3v_{esc}$
R_v	7×10^{11}cm
α	1.5

Table 1. Wind geometry parameters used in the benchmark CV model.

$$v_{\infty} = f v_{esc}, \tag{3}$$

so the innermost streamlines reach the highest velocities. The power-law index α controls the shape of the velocity law: as α increases, the acceleration is increasingly concentrated around $l = R_v$ along each streamline. For large α, the initial poloidal velocity stays low near the disk and then increases quickly through R_v to values near v_{∞}.

Table 1 shows the parameters used in the wind model, and Figure 2 shows a sketch of the geometry of our model, with the key parameters labeled.

4.2 Disk Treatment

Python has has some flexibility when treating the accretion disk as a source of photons, in which the disk is broken down into annuli such that each annulus contributes an equal amount to the bolometric luminosity. Each annulus can be treated either as a blackbody with the corresponding temperature or as a Kurucz stellar atmosphere model (REF) with the appropriate surface gravity and temperature. Both of these methods have flaws. It is known from studies of CV accretion disks that they exhibit absorption cores, which can inpact the overall spectrum even if a wind is present (REF), so the blackbody treatment is not complete. However, the stellar atmosphere models also have problems Wade (1988), and there are clear inconsistencies with using a stellar atmosphere beneath a dense wind region which itself goes some way to simulating the disk atmosphere. Here we use the Kurucz models, partly because they provide the most pessimistic prediction due to the strong absorption beyong the Balmer edge, which is required to be filled in by the recombination emission in the wind (see Section 5.3).

4.2.1 Boundary Layer

Whether we include one, why why not, referring to He II and ionization.

4.3 Synthetic Spectra

Present the spectra.

4.4 Ionization State

Present the ionization state with wind plots showing dominant ions.

5 DISCUSSION OF RESULTS

5.1 The Balmer Series

5.2 UV Resonance Lines

5.2.1 OVI and the Auger effect

5.3 The Balmer Jump

5.4 Helium Lines

5.5 The Line Force

6 CONCLUSIONS AND FUTURE WORK

6.1 Future Work

In addition to this project, we plan to apply the macro atom scheme to QSOs in order to build on the work of Higginbottom et al. (2013), in which a benchmark biconical disk wind model was presented. In particular, we hope that the macro-atom scheme will enable the model to produce significant Lyman-α emission, as is observed in QSOs.

6.2 Acknowledgements

REFERENCES

Badnell N. R., Bautista M. A., Butler K., Delahaye F., Mendoza C., Palmeri P., Zeippen C. J., Seaton M. J., 2005, MNRAS 360, 458
Cordova F. A., Mason K. O., 1982, ApJ 260, 716
Higginbottom N. S., Knigge C., Long K. S., Sim S. A., Matthews J. H., 2013, Submitted to MNRAS
Kerzendorf W. E., Sim S. A., 2014, ArXiv e-prints
Lucy L. B., 2002, A&A 384, 725
Lucy L. B., 2003, A&A 403, 261
Mihalas D. M., 1982, Stellar atmospheres.
Sim S. A., Drew J. E., Long K. S., 2005, MNRAS 363, 615
Wade R. A., 1988, ApJ 335, 394

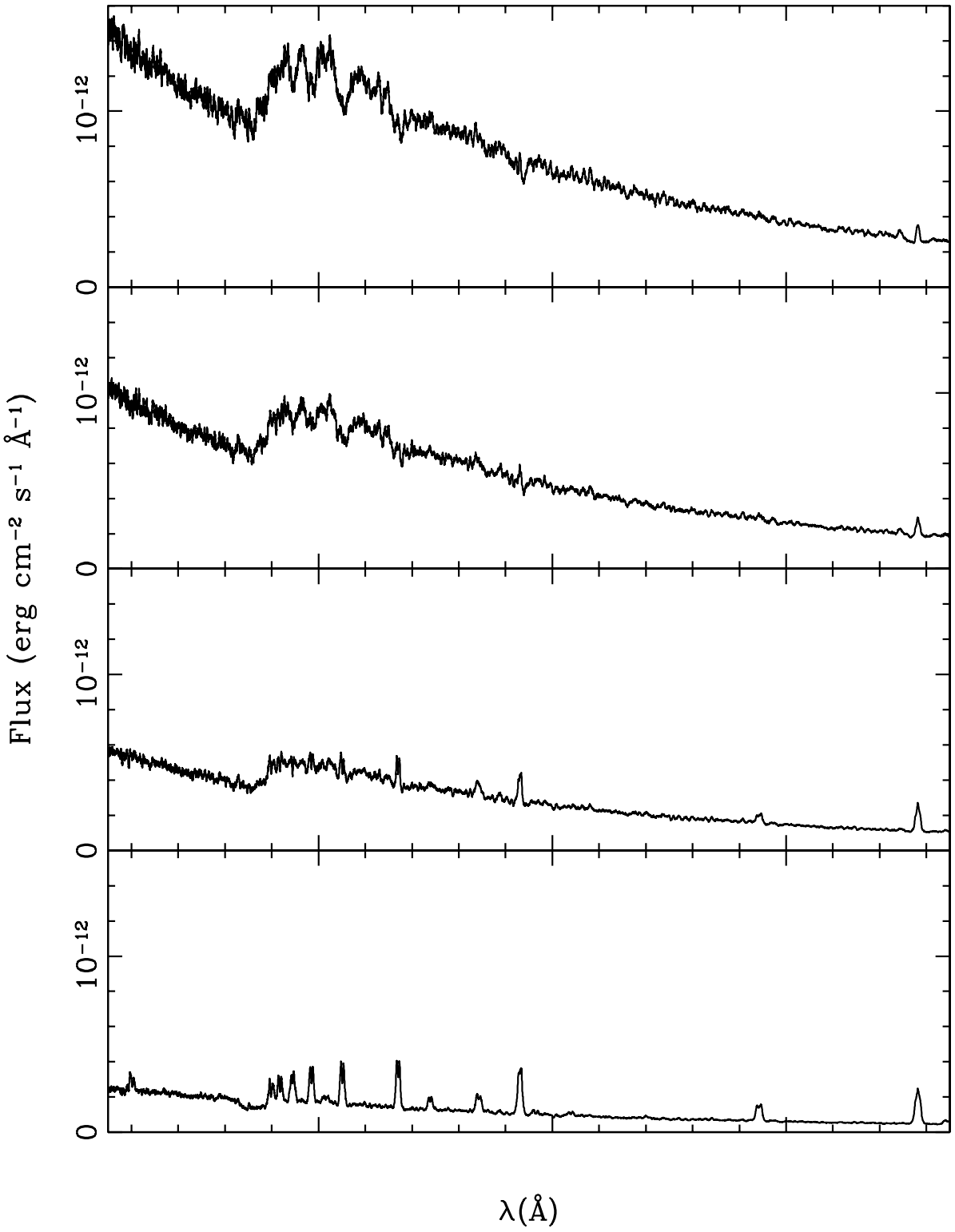

Figure 3. Synthetic Spectra computed for sightlines of 22.5, 25, 62.5 and 80 degrees.